

## REMOTE MEASUREMENT OF ENERGY AND CARBON FLUX FROM WILDFIRES IN BRAZIL

PHILIP J. RIGGAN,<sup>1,7</sup> ROBERT G. TISSELL,<sup>1</sup> ROBERT N. LOCKWOOD,<sup>1</sup> JAMES A. BRASS,<sup>2</sup>  
JOÃO ANTÔNIO RAPOSO PEREIRA,<sup>3</sup> HELOISA S. MIRANDA,<sup>4</sup> ANTÔNIO C. MIRANDA,<sup>4,8</sup>  
TERESA CAMPOS,<sup>5</sup> AND ROBERT HIGGINS<sup>6</sup>

<sup>1</sup>*U.S. Forest Service, Pacific Southwest Research Station, Forest Fire Laboratory, 4955 Canyon Crest Drive, Riverside, California 92507 USA*

<sup>2</sup>*NASA Ames Research Center, Moffett Field, California 94035 USA*

<sup>3</sup>*Instituto Brasileiro do Meio Ambiente e dos Recursos Naturais Renováveis, Brasília DF Brasil*

<sup>4</sup>*Universidade de Brasília, Departamento de Ecologia, Brasília DF Brasil*

<sup>5</sup>*National Center for Atmospheric Research, Atmospheric Technology Division, Boulder, Colorado 80307 USA*

<sup>6</sup>*Simco Electronics, Inc., Moffett Field, California 94035 USA*

**Abstract.** Temperature, intensity, spread, and dimensions of fires burning in tropical savanna and slashed tropical forest in central Brazil were measured for the first time by remote sensing with an infrared imaging spectrometer that was designed to accommodate the high radiances of wildland fires. Furthermore, the first in situ airborne measurements of sensible heat and carbon fluxes in fire plumes were combined with remote measurements of flame properties to provide consistent remote-sensing-based estimators of these fluxes. These estimators provide a means to determine rates of fuel consumption and carbon emission to the atmosphere by wildland fires as required for assessments of fire impacts on regional air pollution or global emissions of greenhouse gases. Observed fires developed complex fire-line geometry and thermal structure, even as average whole-fire temperatures varied little. Flame temperatures sometimes exceeded 1600 K along the leading edge of actively spreading fire lines, yet >90% of the radiant energy from observed fires was associated with temperatures of 830–1440 K. Fire in a partially slashed forest encompassed a high-intensity flaming front and a trailing reach of residual combustion extending 400 m. Fire fronts in tropical savanna typically formed with little depth and a high proportion of their radiant flux density associated with high temperatures due to low levels of residual combustion. Measured fires had such low and variable radiance compared with that of a blackbody of comparable temperature as to preclude the use of fire radiance at a single wavelength as a measure of fire intensity or temperature. One-half of the radiant flux density from a measured savanna fire was associated with values of a combined emissivity–fractional-area parameter <0.091 m<sup>2</sup>/m<sup>2</sup>; for a slash fire this fraction was associated with values <0.37 m<sup>2</sup>/m<sup>2</sup>. Observations reported here show wildland fires to be so complex and dynamic as to require frequent high-resolution measurements over their course and duration in order to specify their effects in the environment; an understanding of global fire impacts may require such measurements over a large sample of individual fires.

**Key words:** carbon flux; Cerrado; extended-dynamic-range imaging spectrometer; fire temperature; heat flux; infrared imaging; radiant flux density; remote sensing; slash fire; tropical forest; tropical savanna; wildfire.

### INTRODUCTION

Fire science and management today are critically limited by an inability to quantitatively measure and track the properties of wildland fires at their full scale and as they occur. Wildfires are by nature shrouded in smoke, difficult and dangerous to approach, sometimes obscured by terrain, and often unpredictable as to location, velocity of propagation, energetics, and environmental impact.

Knowledge of fire properties is needed at scales from the local to the global. Tactical fire suppression requires either tracking or prediction of fire spread rates, intensity, and direction so as to keep personnel and resources from harm's way and maximize their effectiveness. Mitigation of the ecological impacts of fire requires either active monitoring of fire properties or a means to deduce them from an assessment of the burned area, since the impacts may be substantially affected by fire energy release rates or intensity. For example, increased intensity of burning can effect greater nitrogen volatilization, nitrification in soil, and nitrogen flux in stream water (Dunn and DeBano 1977, Riggan et al. 1994), with potential effects on soil productivity and aquatic ecosystems; accelerated soil erosion due to fire-

Manuscript received 16 May 2002; revised 11 April 2003; accepted 9 June 2003; final version received 18 August 2003.  
Corresponding Editor: C. A. Wessman.

<sup>7</sup> E-mail: priggan@fs.fed.us

<sup>8</sup> Deceased.

induced water repellency (DeBano et al. 1977, Wells 1981); higher postfire flood peaks (Riggan et al. 1994); seed destruction or altered germination and postfire recovery (Moreno and Oechel 1994); and altered forest structure from higher rates of canopy consumption or tree mortality (Van Wagner 1973). Avoidance of severe impacts requires strategic planning and an ecosystem analysis that specifies the likely response of a wildfire regime to different levels of intervention by prescribed burning or other means of fuel management. At continental to global scales, wildland fires and agricultural burning are an important source of trace gases and aerosols that pollute the atmosphere and can contribute to global climate change (Crutzen and Andreae 1990). National policy and international protocols to mitigate these impacts depend on reliable estimates of fire emissions including the flux of carbon to the atmosphere.

Here we describe the first applications of remote sensing to the quantitative estimation of fire-line intensity and geometry and the sensible heat and carbon fluxes in plumes from large wildland fires, thereby providing a synoptic view of fire behavior and properties. Our approach has been to evaluate bulk flame temperatures, radiant-energy flux, flaming-front geometry, and rate of areal spread with a specialized, airborne, imaging spectrometer and to estimate carbon and sensible-heat fluxes within fire plumes from in situ airborne measurements of the vertical component of wind velocity, potential temperature, CO<sub>2</sub> mixing ratio, and plume geometry. Such measurements were made for two fires burning in the Cerrado, which is tropical savanna vegetation, and a large slash fire in tropical forest in central Brazil. A method for estimating plume sensible-heat flux from remote sensing measurements of the fire line was consistently and successfully applied to the data from the three fires. Furthermore, we show that plume carbon flux is linearly and well related to sensible-heat flux across a range of wildland and agricultural fires and conditions, and that plume carbon flux, when combined with estimates of areal rate of fire spread, provides useful estimates of fuel consumption rate. From remote sensing alone, these techniques provide a means to assess a number of important fire properties required for fire-behavior modeling, understanding ecological fire effects, and the estimation of global biomass combustion rates and fire emissions to the atmosphere.

## METHODS

### *Measured fires*

We observed two freely burning fires in natural Cerrado vegetation: the Tapera prescribed fire in the late afternoon of 21 September 1992 at the Reserva Ecológica of the Instituto Brasileiro de Geographia e Estatística (IBGE; Ecological Reserve of the Brazilian Institute of Geography and Statistics) in the Brazilian Federal District, as well as a set pasture fire on 15

September 1992 in the Serra do Maranhão, ~65 km north of Brasília. On 22 September 1992, we also measured an active fire burning in partially slashed tropical forest near Marabá, Pará. The latter fire burned in selectively harvested, primary forest.

The Tapera fire burned within a watershed of low relief, ranging from 1040 to 1130 m elevation. Upland vegetation there is comprised of three phases of the Cerrado (campo cerrado, campo sujo, and campo limpo) that are distributed in the order listed from higher to lower elevations. Evergreen shrubs along this plant community gradient comprise a declining proportion of the plant cover in a grassland matrix. Biomass structure in these communities has been described by Ottmar et al. (2001). The fire was ignited by hand-carried drip torches along a trail on the fire's eastern perimeter and adjacent to a narrow gallery forest on the north (Fig. 1). Firing then progressed along the southern firebreak, with ignition keeping pace of the wind-driven fire line. The fire was contained on the west by a narrow burned strip and on the south by a cleared firebreak. We made remote sensing or in situ plume measurements of the Tapera fire over ~45 min from first ignition through the end of active combustion.

The Serra do Maranhão fire was first observed in progress at 1622 hours local time. Observations were made across 80 minutes. The fire burned across elevations of ~800–950 m, with grassland uplands, several phases of Cerrado along some slopes, and gallery forest along stream courses.

The Marabá fire was observed in progress during 1310–1317 hours local time, with a well-developed plume and a strong plume-capping cumulus. The fire had been ignited in selectively harvested primary forest with standing trees and logging slash and in adjacent pasture that had been converted from forest. Local ground elevation is ~250 m.

### *Airborne measurements*

Remote sensing and atmospheric measurements were made from the King Air B200t research aircraft of the National Center for Atmospheric Research (National Center for Atmospheric Research 1990). The aircraft was instrumented for fast-response measurement of atmospheric state variables, CO<sub>2</sub> mixing ratio, concentration of cloud water droplets and aerosol particles, and components of air velocity in three dimensions (Lenschow and Spyers-Duran 1989). The CO<sub>2</sub> mixing ratio was measured with a closed-path Licor model 6262 CO<sub>2</sub> and water analyzer (LI-COR, Lincoln, Nebraska, USA), with corrections applied for ambient temperature and pressure. Sample flow rate was ~0.075 L/s. The aircraft also carried a unique airborne extended-dynamic-range imaging spectrometer (EDRIS) that had been optimized for the quantitative measurement of the high infrared radiances associated with wildfires (Riggan et al. 1993). The EDRIS instrument is a line-scanning remote imager, which is part of an

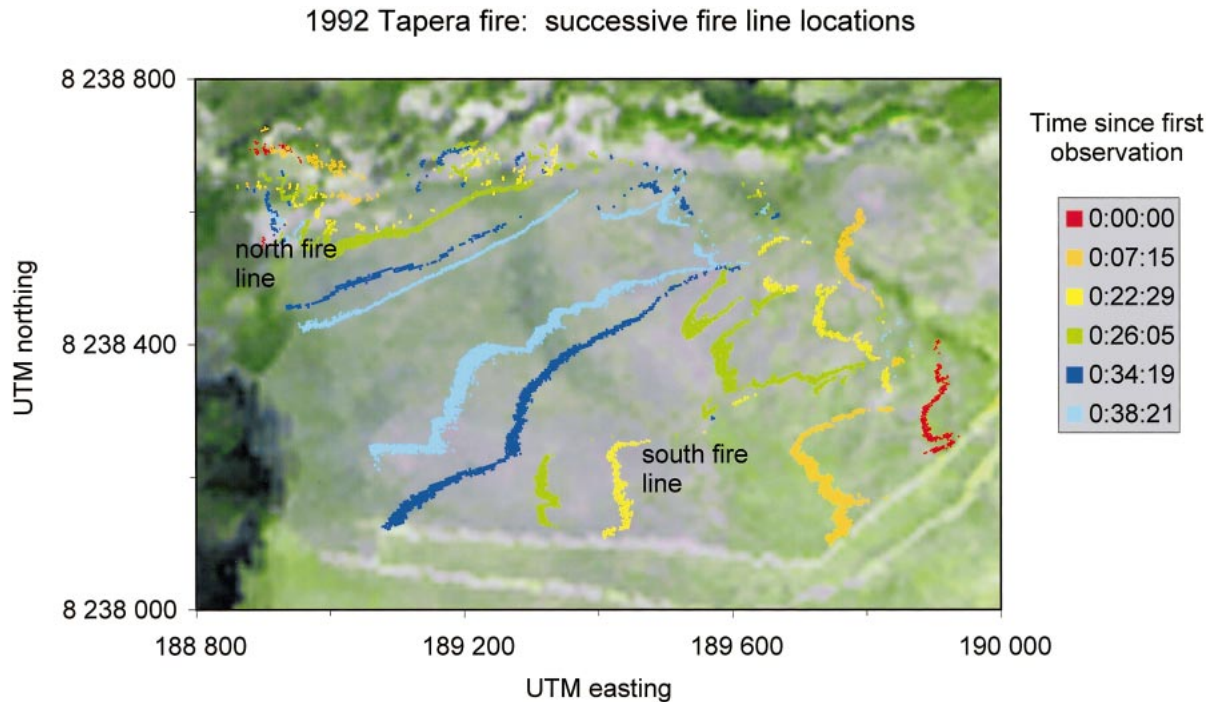


FIG. 1. Successive locations of fire lines for the 1992 Tapera fire, as determined by remote sensing with the extended-dynamic-range imaging spectrometer (EDRIS). Lines are color coded by time since first observation (hours : minutes : seconds [h:min:s]) and mapped on Universal Transverse Mercator (UTM) coordinates. Fire locations are shown on a color composite EDRIS image at wavelengths of 3.9, 0.7, and 1.63  $\mu\text{m}$  (red, green, blue) from 20 August 1994. In this image, areas sparsely covered with grasses appear as light magenta tones. Denser grasses in this rolling terrain appear gray-green, areas with a greater proportion of evergreen shrubs are bright green, and gallery forests appear dark green, as at the top and far left. Parallel light lines at the bottom are cleared firebreaks.

Airborne Infrared Disaster Assessment System developed by NASA Ames Research Center and the U.S. Forest Service.

*Fire remote sensing.*—The EDRIS produces radiance measurements and imagery, digitized to 14 bits, at infrared wavelengths of 1.56–1.69  $\mu\text{m}$ , 3.82–3.97  $\mu\text{m}$ , and 11.5–12.2  $\mu\text{m}$ . These wavelengths were chosen to allow discrimination of flame properties in pixels encompassing both flames and hot ash (Riggin et al. 1993). Spatial resolution of the imager is  $\sim 2.6$  m per 1000 m of altitude above ground level. The infrared channels of the spectrometer were calibrated in the laboratory over a target with estimated emissivity of 0.95 at 1.6  $\mu\text{m}$  and 0.85 at 3.9  $\mu\text{m}$  wavelength and at temperatures spanning 300–860 K. The maximum temperature corresponded to radiances of 347  $\text{J}\cdot\text{m}^{-2}\cdot\text{s}^{-1}\cdot\text{sr}^{-1}\cdot\mu\text{m}^{-1}$  at a wavelength of 1.63  $\mu\text{m}$ , 1566  $\text{J}\cdot\text{m}^{-2}\cdot\text{s}^{-1}\cdot\text{sr}^{-1}\cdot\mu\text{m}^{-1}$  at 3.9  $\mu\text{m}$ , and 154  $\text{J}\cdot\text{m}^{-2}\cdot\text{s}^{-1}\cdot\text{sr}^{-1}\cdot\mu\text{m}^{-1}$  at 11.9  $\mu\text{m}$ . Preamplifiers on the infrared channels were designed with a dual-range response that is linear with high gain at radiances associated with typical terrestrial temperatures and low gain at radiances expected at fire temperatures.

To estimate wildland fire properties by remote sensing, we assumed that the radiant emissions of flames, outside of wavelengths with strong molecular absorption, are dominated by the radiation from glowing soot

particles that act as gray-body radiators with high emissivity. Such radiation is described by the Planck function with parameters of temperature and emissivity, the latter of which relates radiance to that of a perfect blackbody radiator. Flames in biomass fires can be optically thin so that upwelling radiation encompasses radiation from hot soil beneath the flames as well as from the entrained soot particles. For large flames or those of high soot-particle volume, such as found in aviation fuel fires, upwelling radiation can originate from and reflect the temperature of upper flames alone (L. Gritz, *personal communication*). Yet even with long flame lengths, flaming zone turbulence can be so great as to dictate that high-temperature flames occupy only a fraction of a remote-sensing pixel, even for pixels that fall well within a flaming front. The remainder can be composed of residual flaming combustion and smoldering of larger biomass elements, cooling ash, and unburned vegetation. Thus, a parameter representing the product of emissivity and the fractional area of fire within a pixel must be estimated in order to represent fire radiance, and any such pixel can encompass a variety of targets with differing temperatures.

Estimation of the temperature ( $T$ ) of a gray-body radiator and the product of its emissivity ( $\epsilon$ ) and fractional area ( $A_f$ ) within a pixel requires measurement of

the emitted energy from at least two wavelengths,  $\lambda_1$  and  $\lambda_2$  (Riggan et al. 1993, Matson and Dozier 1981). With high spatial resolution in relation to the dimensions of the fire front, it may be assumed that the background radiance from vegetation or ash within a pixel is negligible in relation to that from the flames, so the background can be ignored (Riggan et al. 2000). Planck functions for the apparent flame radiances ( $B_1$  and  $B_2$ ) at two wavelengths can then be solved simultaneously to yield the following relations:

$$T = \frac{hc}{k\lambda_1 \ln \left\{ \left( \frac{B_2}{B_1} \right) \left( \frac{\lambda_2^5}{\lambda_1^5} \right) \left[ \exp \left( \frac{hc}{k\lambda_2 T} \right) - 1 \right] + 1 \right\}} \quad (1)$$

$$\varepsilon A_f = \frac{B_i \lambda_i^5 \left[ \exp \left( \frac{hc}{k\lambda_i T} \right) - 1 \right]}{2 \times 10^{-6} hc^2} \quad (2)$$

where  $h$  is the Planck constant ( $6.63 \times 10^{-34}$  J·s),  $c$  is the speed of light ( $3.00 \times 10^8$  m/s),  $k$  is the Boltzmann constant ( $1.38 \times 10^{-23}$  J/K),  $T$  is specified in Kelvin,  $\lambda$  is in meters,  $B_\lambda$  has units of joules per square meter per second per steradian per micrometer ( $\text{J}\cdot\text{m}^{-2}\cdot\text{s}^{-1}\cdot\text{sr}^{-1}\cdot\mu\text{m}^{-1}$ ), and radiances are corrected for atmospheric transmittance. Eq. 1 can be solved iteratively to yield  $T$ , and the product  $\varepsilon A_f$  can be computed from either wavelength via Eq. 2. Note that temperature estimation is independent of emissivity and fractional area. The wavelength-integrated radiant flux density,  $F_d$  ( $\text{J}\cdot\text{m}^{-2}\cdot\text{s}^{-1}$ ), which is a measure of fire intensity, is given by

$$F_d = \varepsilon A_f \sigma T^4 \quad (3)$$

where  $\sigma$  is the Stefan-Boltzmann constant ( $5.67 \times 10^{-8}$   $\text{J}\cdot\text{m}^{-2}\cdot\text{s}^{-1}\cdot\text{K}^{-4}$ ; Liou 1980). We simulated atmospheric transmittance over measured fires with a medium-resolution spectral model, MODTRAN, using measured atmospheric water vapor, temperature, and pressure. No corrections for smoke aerosols were made, since these are expected to have little impact on transmittance at these infrared wavelengths (Riggan et al. 1993), and the observation geometry here was such that flaming fronts were generally observed to the side of inclined smoke plumes.

*Areal fire growth.*—Multispectral eight-bit imagery of the fires was registered to a common base using the MicroImage software of TerraMar Resources. For the Tapera fire, this base consisted of a 1:10 000-scale topographic survey of the Reserva Ecológica provided by IBGE. For the Marabá slash fire, we used as a base a prefire Landsat Thematic Mapper scene from 10 August 1992. For the Serra do Maranhão fire, we used digital aerial photography collected in August 2000. Geo-referenced locations of the original 14-bit fire radiance data were determined by applying transformation equations from the initial registrations to line and

sample numbers in the original data sets. Sizes for each high-temperature pixel were determined from the transformation equations by calculating differences in Universal Transverse Mercator (UTM) coordinates between that pixel and offsets of a single line and sample number. Areal growth of the fire was estimated by planimeter for areas between the registered images of successive fire-line observations. Times for successive remote-sensing passes were taken from times of closest approach to the fire, as recorded by the aircraft navigation system.

*In situ measurement of heat and carbon flux in fire plumes.*—Fluxes of sensible heat and  $\text{CO}_2$  were concurrently estimated in cross sections through upwelling portions of each fire plume. Plume measurement transects during the Tapera and Marabá fires were generally flown with the ambient wind field; transects through the Serra do Maranhão plume were largely perpendicular to the ambient wind. We analyzed 25-Hz data for the vertical component of wind velocity, potential temperature, and  $\text{CO}_2$  mixing ratio to estimate plume sensible heat and carbon fluxes. Carbon dioxide data were offset in time to account for a 1.76-s lag behind the vertical wind measurements.

Instantaneous fluxes,  $F_s$ , at a given height in the plume above ground, were defined as

$$F_s \equiv \rho w' s' \quad (4)$$

where  $\rho$  is the dry-air density,  $w$  is the vertical component of air velocity,  $s$  represents the mass mixing ratio with respect to dry air for fluxes of substances such as water or  $\text{CO}_2$ , and the prime denotes an instantaneous deviation from mean ambient values. Heat flux was similarly given as

$$Q_s \equiv \rho_{\text{air}} C_p w' \theta' \quad (5)$$

where  $\theta$  is potential temperature of the air, and  $\rho_{\text{air}}$  is the density and  $C_p$  is the specific heat of moist air. We estimated the whole-plume fluxes from the product of plume cross-sectional area and mean values of  $F_{\text{CO}_2}$  and  $Q_s$  from transects within the plume. The mean ambient-air vertical velocity was assumed to be zero, and mean ambient-air  $\text{CO}_2$  mixing ratio and potential temperature were taken as the mean from a flight segment immediately preceding plume entry. Aircraft sensors estimate the flux at the altitude of the aircraft, so transects were made as low as practicable to approximate the surface fluxes. This approximation should be adequate, especially for fires with nearly steady rates of spread and plumes with limited low-level divergence and high vertical velocities. Sampling altitudes above ground level were  $\sim 180$ – $250$  m at the Tapera fire,  $1200$ – $1340$  m at the Serra do Maranhão fire, and  $500$ – $1830$  m at the Marabá fire.

*Estimates of areal fuel consumption.*—For fire complexes with short residence times spreading at a nearly steady state, as in tropical savanna, energy or carbon flux per unit area burned can be estimated for intervals

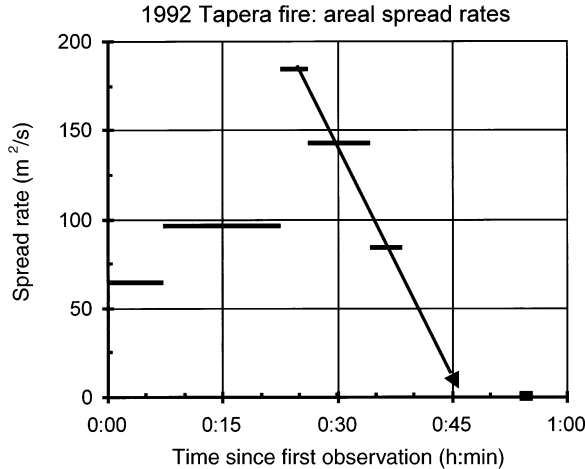


FIG. 2. Rates of areal spread for the 1992 Tapera fire, as computed from fire-line position during successive remote-sensing observations as in Fig. 1. The approximate time at which the final fire size was obtained was estimated by extrapolation (arrow). The final observation of the fire area was at 16:30 in the afternoon, local time.

of minutes to hours from the ratio of the corresponding whole-fire rates and the associated areal progression of the fire over the interval. That is,

$$\frac{dC}{dA} = \frac{\tilde{F}_C}{dA/dt} \quad (6)$$

where  $dC/dA$  (in units of kilograms per square meter) is the fuel carbon consumption rate,  $\tilde{F}_C$  is the instantaneous whole-plume carbon flux rate (in kilograms per second), and  $dA/dt$  (in square meters per second) is the areal spread rate of the fire. Here we considered the carbon flux from that of  $\text{CO}_2$  alone. Areal progression is readily estimated from the growth of the ash layer from successive, geo-referenced images. Estimates of consumption rate for fires with residence time longer than the interval between successive observations, as expected for fires in slashed forest or organic soils, require integration of a time course of carbon or energy flux over the life of the fire.

#### Ground-level measurements at the Tapera fire

Air temperatures were measured with unshielded 30 AWG chromel/alumel thermocouples (Omega Engineering, Stamford, Connecticut, USA) at heights of 1, 30, 60, and 160 cm above the soil surface at two locations within the fire area. Campbell CR-21× data loggers (Campbell Scientific, Logan, Utah, USA) recorded observations at a frequency of 1 Hz during burning. Consumable fuel in the campo limpo plant community was estimated before burning by clipping, drying, and weighing biomass in 25, 0.25-m<sup>2</sup> plots (Dias 1994). Ground-level measurements were not possible at either the Serra do Maranhão fire or Marabá slash fire, since these were observed as targets of opportunity and were not planned research fires.

## RESULTS

### Tapera fire

The Tapera fire spread with two primary fire lines burning in similar vegetation: one parallel to the ambient wind and spreading at only 0.1 m/s (the north fire line) and one with portions spreading largely down slope with the wind (the south fire line; Fig. 1). Flames on the north line were observed to lie over the fire line itself, rather than over unburned fuel in the direction of spread. The south fire line, which accounted for most of the area burned by the fire, initially consisted of several lobed fronts; these eventually merged into a single line running diagonally to the mean wind. Specification of linear rates of spread for the south line is somewhat problematic because of its irregular shape. Once established, lobes of the south fire line traveled at 0.3–0.7 m/s in the direction of the mean wind (Fig. 1). Areal rates of spread are more quantifiable: For the south fire line, these ranged from 65 m<sup>2</sup>/s during early observations to a peak of 185 m<sup>2</sup>/s (Fig. 2). Areal spread rates declined as the fire encountered heavier biomass loading near the watercourse at the western boundary of the watershed and as the leading edge of the fire line reached the project boundary ~34 min after first observation. The Tapera fire ultimately encompassed 49 ha.

For the Tapera fire, estimates of atmospheric transmittance using MODTRAN were 0.97 at a wavelength of 1.63  $\mu\text{m}$  and 0.95 at 3.9  $\mu\text{m}$ ; radiance corrections for these values at a remote-sensing altitude of 1 km above ground level resulted in a fire temperature correction of only 5 K.

Mean radiometric flame temperatures for the Tapera fire as a whole varied little from early to late stages of the fire (Table 1), although there were strong temperature gradients across and along various portions of the line as they became active (Fig. 3). Flame temperatures exceeded 1600 K along portions of the leading edge of actively spreading fire lines. Fire temperatures at the interior of active lines were commonly in the range 900–1200 K. The trailing edge represented reaches of residual combustion with mean temperatures <900 K. There were no consistent differences over time between

TABLE 1. Progression of radiometric flame temperature with time during the Tapera fire.

| Time since first observation | Flame temperature (K) |      |
|------------------------------|-----------------------|------|
|                              | Mean                  | 1 SD |
| 0:00:00                      | 1107                  | 139  |
| 0:07:15                      | 1122                  | 135  |
| 0:22:29                      | 1114                  | 142  |
| 0:26:05                      | 1097                  | 164  |
| 0:34:19                      | 1124                  | 127  |
| 0:38:21                      | 1125                  | 184  |

Note: The first observation was at 15:35:11 local time, where time units are given in terms of hour: minutes: seconds (h:min:s).

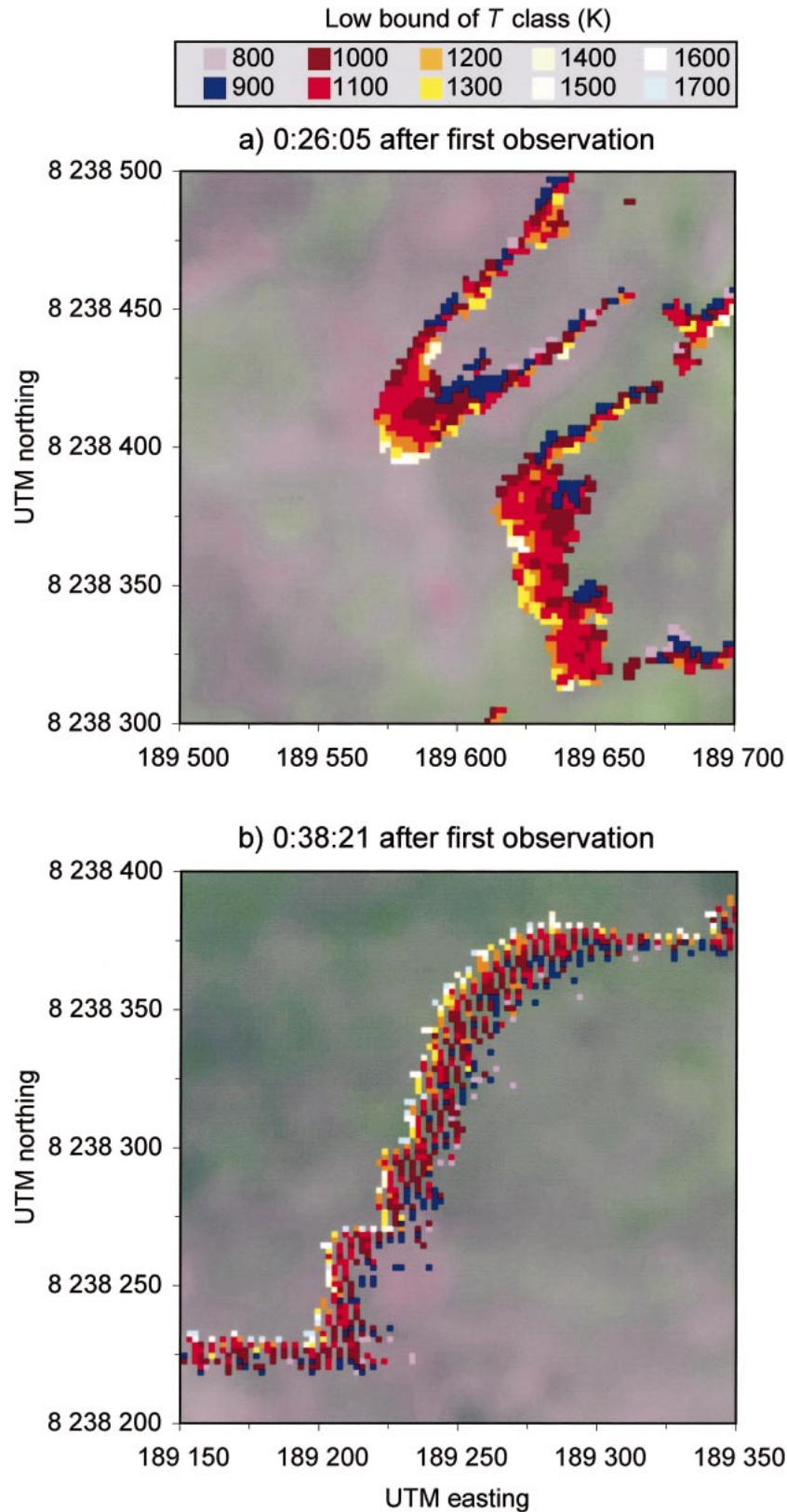


FIG. 3. Map of radiometric temperatures for wind-driven segments of fire line at the 1992 Tapera fire: (a) with pixel spacing of  $\sim 3.1$  m, as remotely sensed from 1050 m above ground; and (b) with scan line spacing of 3.1 m and pixel spacing within lines of 0.8 m, as remotely sensed from 200 m above ground. Time after first observation is expressed as h:min:s. Fire spread is toward the (a) southwest and (b) west. The image background is as in Fig. 1.

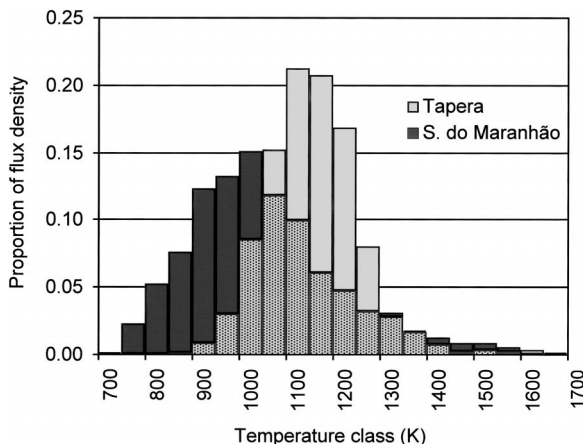


FIG. 4. Distribution of radiant flux density by temperature for the Tapera fire at 16:09:30 (0:34:19 after first observation) and Serra do Maranhão fire at 16:22:15 (0:03:45 after first observation). The area of stippling in the figure shows overlap between the two histograms. The relatively high proportion of flux density at lower temperatures in the Serra do Maranhão fire reflects the importance there of large areas of residual combustion, as shown in Fig. 8.

mean temperatures of the narrow north fire line, which spread laterally to the wind, and the broader south line, which generally spread with the wind.

Ninety percent of the primary fire line's radiant energy flux at its peak (0:34:19 [h:min:s, i.e., hours : minutes : seconds] after first observation) was associated with temperatures in the range 1004–1315 K (Fig. 4). One-half of the radiant flux density occurred at temperatures <1152 K.

The Tapera fire line was observed from different altitudes only on successive passes, so no observations were made in which sampling resolution was not confounded with time. Nonetheless, there were similar patterns and gradients in temperature across the primary fire line when it was observed from 1084 m altitude (for example, at 0:26:05 after first observation) and from 220 m altitude (at 0:38:21 after first observation; Fig. 3). Radiant flux density at temperatures >1150 K was equivalent (less than one percent difference) between these two observations, but at the latter time radiant flux density associated with temperatures <1150 K was approximately twice that from the earlier time.

Mean peak temperature registered by thermocouples near the ground surface within the area of the fire was 827 K (1 SD = 118,  $n = 6$ ); the greatest value recorded, 1061 K, was well within the range of flame temperatures estimated by remote sensing.

The emissivity–fractional-area parameter from Eq. 2 attained low values overall, even within the interior of fire lines where it was generally the greatest. The lowest values of this parameter were associated with the highest recorded temperatures at the leading edge of fire lines and with the residual combustion at the trailing

side of fire lines (Fig. 5). At the leading edge this is likely due to heterogeneity in the wind-driven flame front and the inclusion in the pixel of unburned ground ahead of the fire. Ninety percent of the radiant flux density for the rapidly spreading south line at its peak was associated with values of  $\varepsilon A_f$  in the range 0.017–0.26  $\text{m}^2/\text{m}^2$ . One-half of the radiant flux density was associated with values <0.091  $\text{m}^2/\text{m}^2$ .

There was little residual combustion behind the upland fire lines of the Tapera fire, and after passage of the flaming front the soil surface radiated little energy at the short and intermediate infrared wavelengths measured. Cooled ash and unburned ground showed radiances at 1.63  $\mu\text{m}$  that were only one to two percent of values observed in the flaming zone and thus contributed insignificantly to the signal from any pixel encompassing flaming combustion.

Combustion within the southern line of the Tapera fire formed an inclined primary emission plume that extended through the 1.6-km depth of the atmospheric boundary layer. The slowly propagating northern fire line and nearby residual burning formed a smaller secondary plume near ground level that was not sampled.

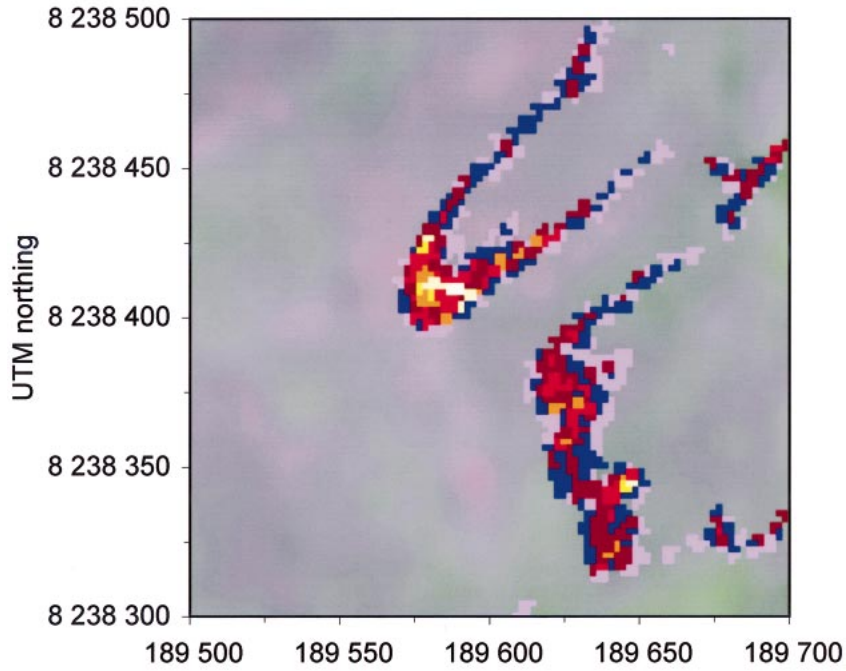
Vertical air velocities ( $w_v$ ) within the primary plume were readily discriminated from those in the ambient wind field; vertical wind shear as great as 15 m/s in the plume was measured over a horizontal distance of 40 m (Fig. 6). Combined with a strong elevation of the  $\text{CO}_2$  mixing ratio, which peaked at 802  $\mu\text{L}/\text{L}$ , these velocities produced a plume carbon flux as great as  $2.7 \times 10^{-3} \text{ kg}\cdot\text{m}^{-2}\cdot\text{s}^{-1}$ , more than three orders of magnitude greater than local peak values typical of ambient air (Fig. 6). Potential air temperature in the plume at the altitude sampled was as much as 4 K greater than that of the ambient air (Fig. 6). This elevation, together with the positive vertical air velocities, resulted in a strong heat flux signal. Carbon and sensible-heat fluxes were also horizontally stratified in the lower plume, with highest rates located on the upwind, eastern side (Fig. 7).

Maximum downwind extent of the plume at the altitude sampled, which we defined by substantial reaches of carbon flux  $>5 \times 10^{-5} \text{ kg}\cdot\text{m}^{-2}\cdot\text{s}^{-1}$ , was  $\sim 690$  m. Plume width, measured as the width of the south line perpendicular to the mean wind, was 265 m. An independent estimate of 285 m at 250-m altitude was derived from remote sensing of the plume with consideration of plume inclination and image distortion from line-of-sight projection of the elevated plume onto the ground surface. By assuming an elliptical plume cross section parallel to the ground with major axis of 690 m and minor axis of 275 m and applying average measured fluxes across this area (as in Fig. 7), we estimated an instantaneous carbon flux for the entire south line of the Tapera fire of 29 kg/s and a sensible-heat flux of  $8.7 \times 10^8$  J/s (Table 2). Assuming that carbon makes up one-half of the consumed biomass, the carbon flux and average areal spread rate ( $54 \text{ m}^2$

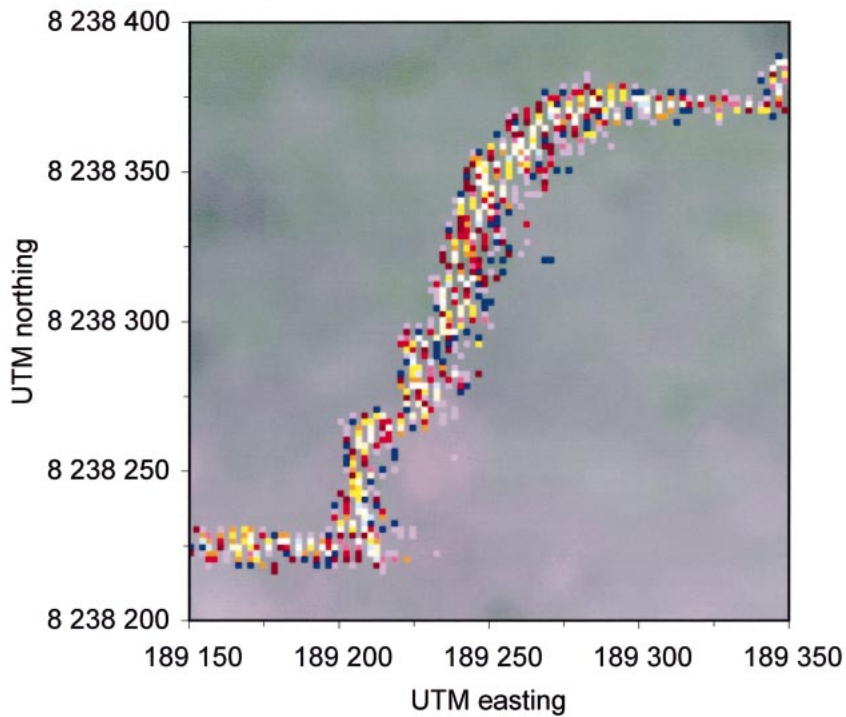
Low bound of  $\epsilon$ - $A_f$  class ( $m^2/m^2$ )



a) 0:26:05 after first observation



b) 0:38:21 after first observation



s) from the latter period of plume sampling give an average fuel consumption estimate for the active south fire line of  $1.1 \text{ kg/m}^2$ .

#### *Serra do Maranhão fire*

The Serra do Maranhão fire was first observed well in progress as a complex of hot flaming fronts in grasses and large reaches of cooler, residual combustion in heavier woody fuels (Fig. 8). It produced a substantial cumulus-capped plume beneath a cover of stratocumulus. A wide range in fire activity was observed over the course of 72 min of observation as fire fronts flared, spread and merged, or remained nearly stationary (Fig. 9). The large, persistent reaches of residual combustion were most remarkable in comparison with other fires we have observed in the Cerrado region. Discernable linear spread, at rates of  $0.02 \text{ m/s}$  perpendicular to the wind and of  $0.03 \text{ m/s}$  with the wind, was primarily in grasses where fire lines were narrow, encompassing a width of one to three pixels at  $10\text{-m}^2$  resolution. Areal spread was only  $37 \text{ m}^2/\text{s}$  (a total of 16 ha) over the period of observation. At last observation, the Serra do Maranhão fire had reached an area of 59 ha.

As with the Tapera fire, the spatially averaged radiometric flame temperatures of the Serra do Maranhão fire varied little across 72 min of observation (Table 3), even though there were considerable local changes in activity as different fuel types became engaged. Overall, 90% of the fire radiant flux density (for example, at 0:03:45 after first observation) occurred within the temperature range  $830\text{--}1383 \text{ K}$ . One-half of the flux density occurred below a temperature of  $1032 \text{ K}$ . The greater fraction of overall fire radiance at relatively low temperatures (Fig. 4), in comparison with the Tapera fire, apparently resulted from the much greater area of residual combustion in the Serra do Maranhão fire.

The Serra do Maranhão fire formed primary and secondary plumes (Fig. 10); the primary plume was stable and persistent over the period of sampling. The primary plume, which was inclined  $29^\circ$  from the vertical, reached through the  $4300 \text{ m}$  depth of the atmospheric boundary layer to form a capping cumulus that peaked at an altitude of  $5100 \text{ m}$ . The plume widths at  $1280 \text{ m}$  above ground were  $690 \text{ m}$  crosswind and  $790 \text{ m}$  with the wind, which yield an estimated cross-sectional area of  $4.3 \times 10^5 \text{ m}^2$ . The peak vertical component of air velocity within the plume was  $8.8 \text{ m/s}$ . As with the Tapera fire, the highest carbon fluxes within the plume were on the upwind side. Whole-plume carbon flux, estimated from the product of cross-sectional area and

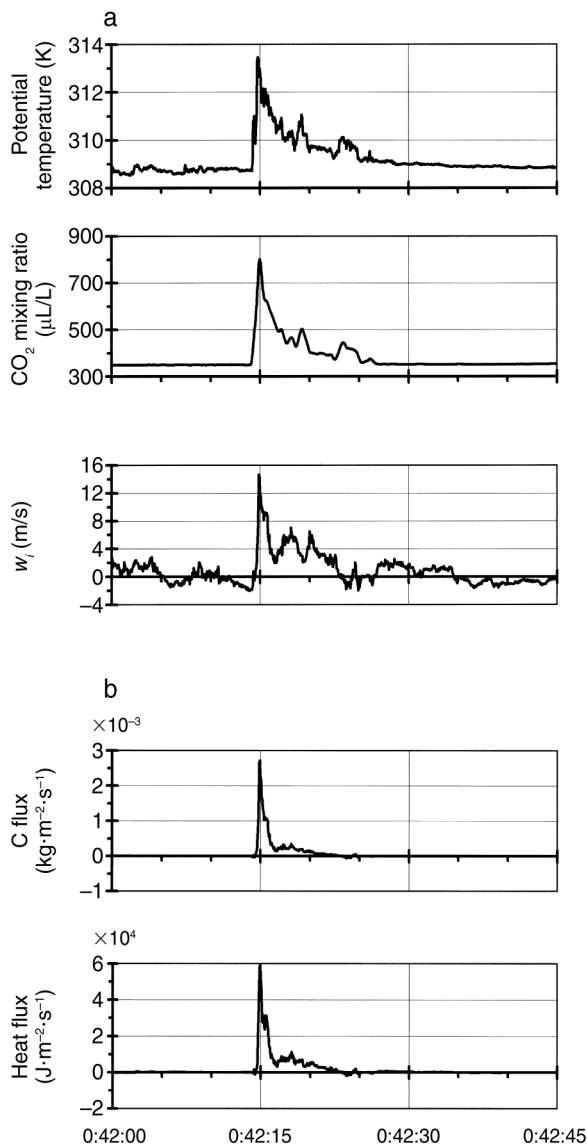


FIG. 6. (a) Measured potential temperature, CO<sub>2</sub> mixing ratio, and vertical air velocity ( $w_v$ ) along a transect at  $\sim 180 \text{ m}$  altitude above ground within the plume of the Tapera fire. (b) Carbon and heat fluxes are estimated from variables shown in (a). Values on the x-axis indicate time since first observation (h:min:s).

average measured carbon flux for each of the primary and secondary plumes, was  $47 \text{ kg/s}$ .

#### *Marabá slash fire*

The fire in partially felled tropical forest at Marabá (Fig. 11) was ignited along the northern and upwind,

←

FIG. 5. Map of the emissivity–fractional-area parameter for segments of fire line at the 1992 Tapera fire, with distinctions between parts (a) and (b) as in Fig. 3. This parameter obtained generally low values throughout the fire line even at high resolution; thus, fire radiant flux density appears low compared to that of a blackbody at comparable temperature.

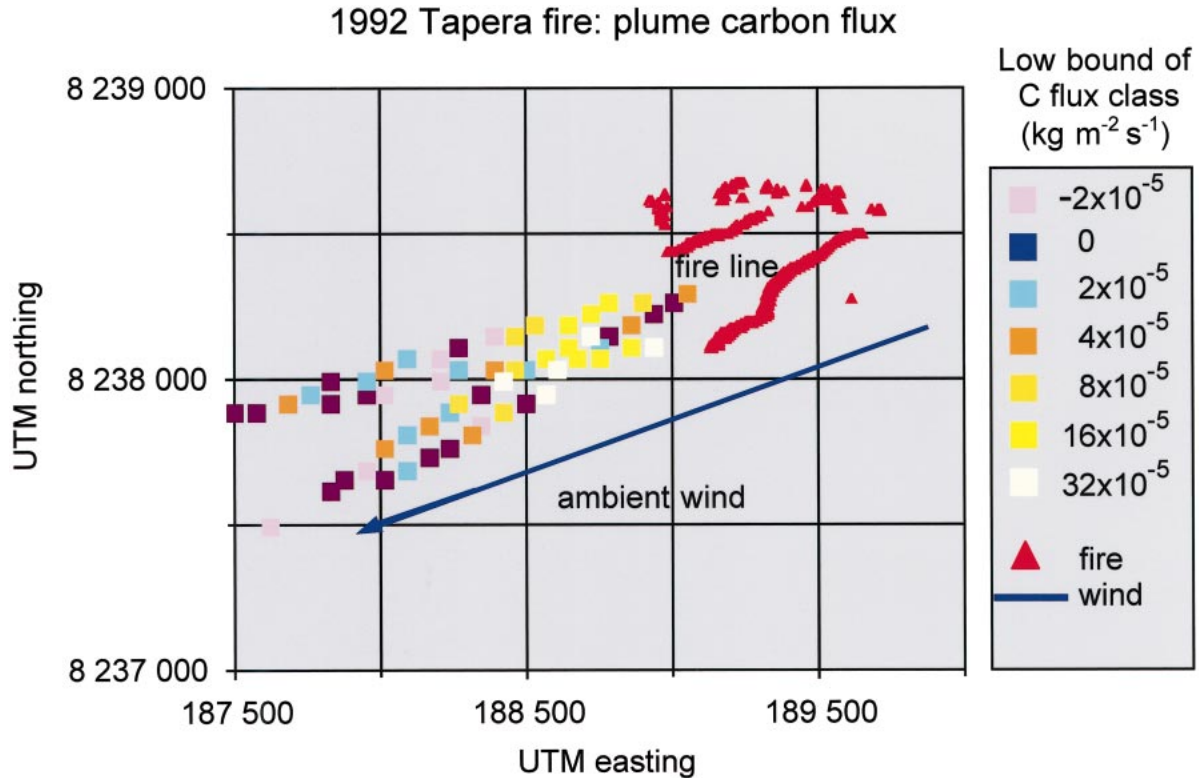


FIG. 7. Plume carbon flux as mapped from cross-plume airborne measurements of the 1992 Tapera fire. Instantaneous measurements are color coded by flux rate and mapped on Universal Transverse Mercator coordinates derived from the aircraft navigation system. Also depicted is the direction of the average ambient wind at 300 m above ground and the position of the fire line at the beginning of four lengthwise plume transects. The low bound of carbon flux progresses as follows:  $-2 \times 10^{-5}$ ,  $0$ ,  $2 \times 10^{-5}$ ,  $4 \times 10^{-5}$ ,  $8 \times 10^{-5}$ ,  $16 \times 10^{-5}$ ,  $32 \times 10^{-5}$  kg·m<sup>-2</sup>·s<sup>-1</sup>.

eastern margins of the harvested area; most of the observed activity resulted from a wind-driven fire front (Fig. 12). The fire involved a wide reach of residual combustion extending as far as 400 m behind the high-temperature front. This residual combustion apparently had a strong effect on the overall distribution of radiant energy flux with temperature. Thus, in comparison with

the Tapera fire in Cerrado vegetation, which showed little residual combustion and a narrow flaming front, a much greater proportion of the radiant flux density from the slash fire was associated with low temperatures than high (Fig. 13). Specifically, 17% of the radiant flux density of the slash fire was associated with temperatures >1075 K; only 17% of that from the Tap-

TABLE 2. Comparison of sensible-heat flux (SHF) estimates, as derived from remotely sensed fire properties and from cross-plume airborne measurements.

| Measurement or estimate                                     | Cerrado           |                                     | Tropical forest                     |
|---|-------------------|-------------------------------------|-------------------------------------|
|   | Tapera fire       | Serra do Maranhão fire              | Marabá slash fire                   |
| Radiant flux density (J/s) from remote sensing measurements |                   |                                     |                                     |
| <i>T</i> > 1100 K   | $4.1 \times 10^7$ | $6.4 \times 10^7$                   | $2.8 \times 10^8$                   |
| All temperatures  | $5.1 \times 10^7$ | $1.6 \times 10^8$                   | $2.4 \times 10^9$                   |
| Modeled from remote sensing                                 |                   |                                     |                                     |
| SHF (J/s) from fire radiance                                | $8.7 \times 10^8$ | <b><math>1.4 \times 10^9</math></b> | <i><math>6.4 \times 10^9</math></i> |
| Plume measurements  |                   |                                     |                                     |
| SHF (J/s)   | $8.7 \times 10^8$ | <b><math>1.4 \times 10^9</math></b> | <i><math>6.7 \times 10^9</math></i> |

Notes: Radiant flux density is shown for comparison. The proportionality constant ( $k_r$ ; Eq. 7 and text immediately following) was determined by setting the remote-sensing-based estimate for the Tapera fire equal to that from airborne measurements; the resultant model was applied to remote-sensing data from the Serra do Maranhão and Marabá fires (compare boldface and italic entries).

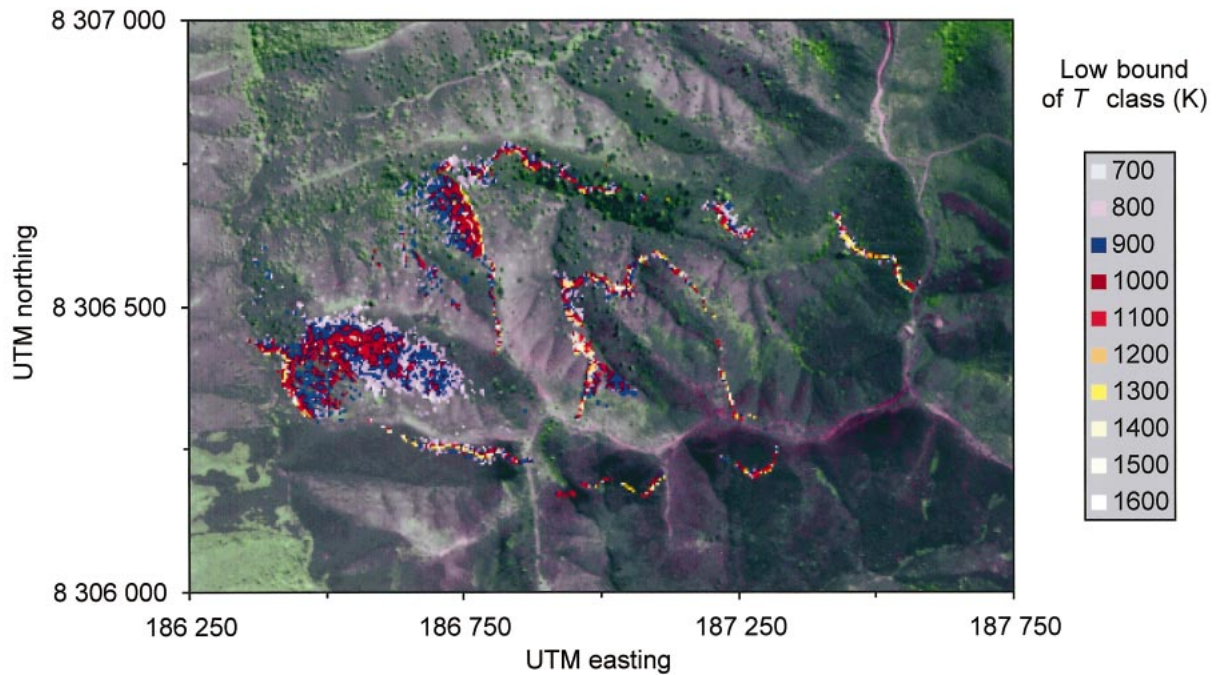


FIG. 8. Temperature map of a freely burning wildland fire in Cerrado vegetation in the Serra do Maranhão, Federal District, Brazil (1992). Radiometric temperatures are at 0:03:45 after first observation. Fire pixels are color coded by temperature class and shown on a background derived from an image of reflected red light at  $0.65 \mu\text{m}$  and near-infrared light at  $0.85 \mu\text{m}$  wavelength that was collected 15 September 2000. Evergreen Cerrado vegetation is shown in light green; dry grassland and bare ground are depicted in magenta tones. Universal Transverse Mercator coordinates are shown. The fire extends  $\sim 1.2$  km from west to east. Note the extended regions of relatively cool residual combustion in the west of the fire and the hot, thin fire lines in grasses, for example, at center and in the northeast.

era fire was associated with temperatures *below* that point. Ninety percent of the radiant flux density from the slash fire occurred within the range 857–1166 K. Nonetheless, that fire was marked by a highly energetic, high-temperature spreading front. When first observed, the fire had encompassed 43 ha; it further grew by 5.7 ha over the ensuing 256 s.

The plume from the Marabá fire showed strong vertical air movement with a peak velocity of 15.4 m/s and a vertical shear of 20.4 m/s over a distance of 63 m. At last observation, the plume was capped by a deep cumulus. The peak value of the  $\text{CO}_2$  mixing ratio, 589  $\mu\text{L/L}$ , was nearly coincident with the maximum vertical air velocity encountered. The resultant maximum instantaneous carbon flux was  $1.2 \times 10^{-3} \text{ kg}\cdot\text{m}^{-2}\cdot\text{s}^{-1}$ . Potential air temperature in the plume at 526 m above ground was as much as 2.4 K greater than in the ambient air. Crosswind width of the plume, as determined from remote sensing of the active fire line, was  $\sim 740$  m; aircraft penetration of the plume yielded a length of 1760 m in the direction of the wind. From these values, we estimated an elliptical cross-sectional area for the inclined plume of  $9.3 \times 10^5 \text{ m}^2$ , an instantaneous whole-plume carbon flux of 234 kg/s, and sensible-heat flux of  $6.7 \times 10^9 \text{ J/s}$ .

#### Flux estimates from remote sensing

We derived estimators of whole-plume sensible-heat flux and carbon flux by relating in situ plume measurements to remotely sensed fire properties. As given in Eq. 5, the heat flux at the top of the combustion zone can be estimated as the product of the kinematic heat flux,  $w'\theta'$ , and the density and specific heat of the air. Here we parameterized the kinematic heat flux as

$$w'\theta' = -K_H \frac{\partial\theta}{\partial z} \quad (7)$$

and assumed the scalar  $K_H$ , the eddy diffusivity (Stull 1988), to be proportional to flame temperature, i.e.,  $K_H = k_T T$ ; the potential temperature gradient,  $\partial\theta/\partial z$ , was taken as proportional to the difference between the temperature of flames and that of the overlying ambient air; and flame temperature and spatial dimensions were estimated by remote sensing. We applied Eqs. 5 and 7, along with these assumptions, to the remotely sensed flame temperatures and emissivity–fractional-area parameters from the south line of the Tapera fire to find the value of the proportionality constant  $k_T$  that obtains a heat-flux estimate equivalent to that derived from in situ plume measurements. The estimate from remote

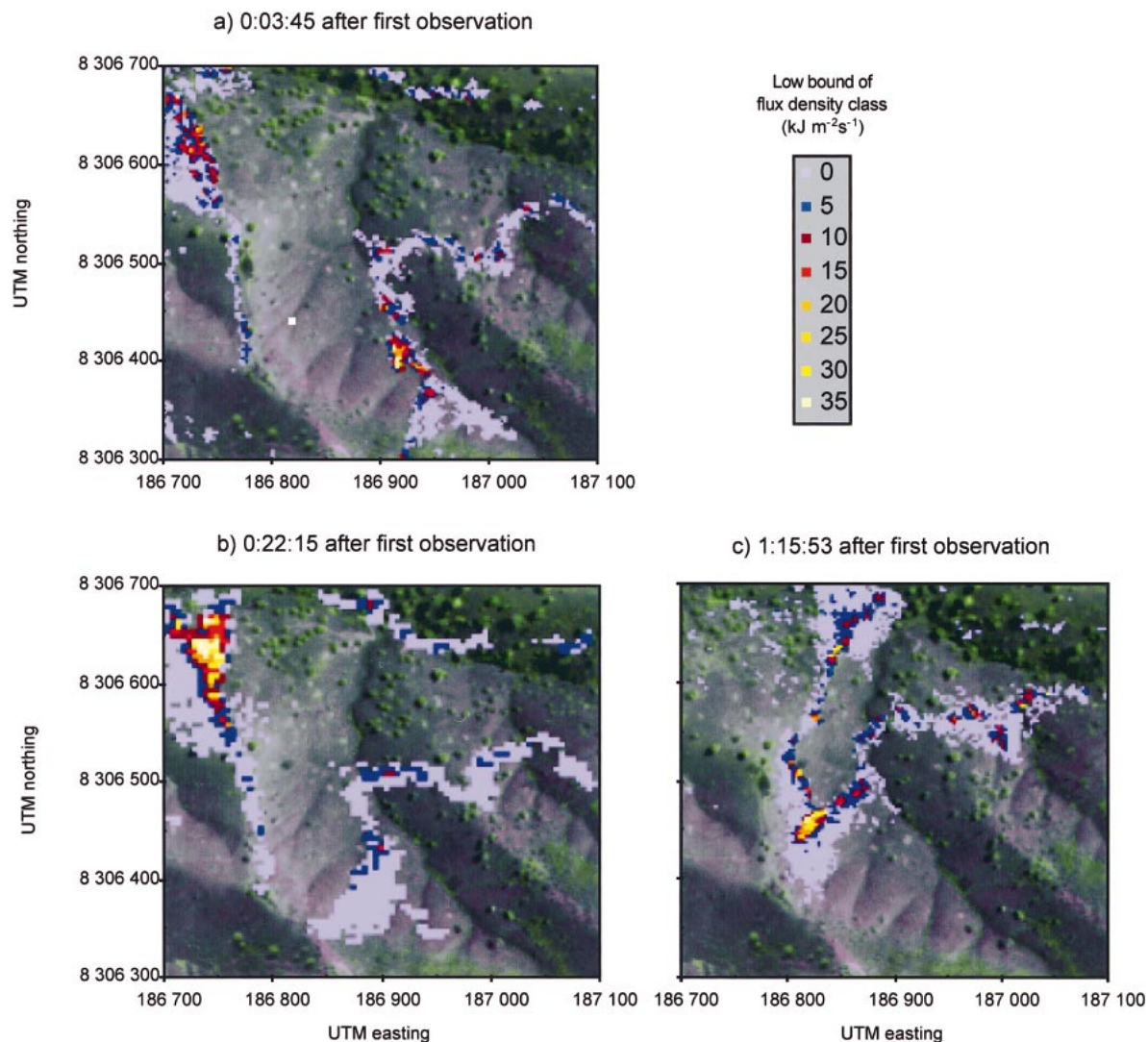


FIG. 9. Time sequence of radiant flux mapped from a portion of the 1992 Serra do Maranhão fire as in Fig. 8. Times are given as h:min:s since first observation at 16:18:30 local time. The distance across the graph is 400 m. Note the changes in energy output or intensity of the fire as the line at the upper left spreads to the east and as two lines merge at the bottom center. The background image is the same as in Fig. 8.

sensing was limited to regions of intense flaming combustion by including in the summation only those pixels with temperatures  $>1100$  K. A value of  $k_r = 0.0026$  resulted.

We tested this model by applying it to remotely sensed temperatures and emissivity–fractional-area parameters of both the Serra do Maranhão and Marabá slash fires. Heat flux estimates from the model, based on remotely sensed properties alone and the proportionality constant derived from the Tapera fire, were nearly equivalent to estimates from in situ plume measurements (Table 2). Furthermore, for a series of aircraft transects through active fire plumes, we found carbon flux to be well and linearly related to sensible-heat flux (Fig. 14). Thus, we have a provisional yet promising method for estimating both sensible-heat

flux and carbon flux to the atmosphere based solely on remotely sensed variables. For fire fronts in which flaming consumption of fuel within an observed pixel is complete within the period of successive observations,

TABLE 3. Progression of mean fire temperature with time during the Serra do Maranhão fire.

| Time since first observation | Flame temperature (K) |      |
|------------------------------|-----------------------|------|
|                              | Mean                  | 1 SD |
| 0:03:45                      | 1007                  | 163  |
| 0:14:44                      | 1011                  | 157  |
| 0:22:15                      | 1017                  | 149  |
| 1:15:53                      | 1006                  | 170  |

*Note:* The first observation was at 16:18:30 local time, where time units are given in terms of h:min:s.

## 1992 Serra do Maranhão fire: plume carbon flux

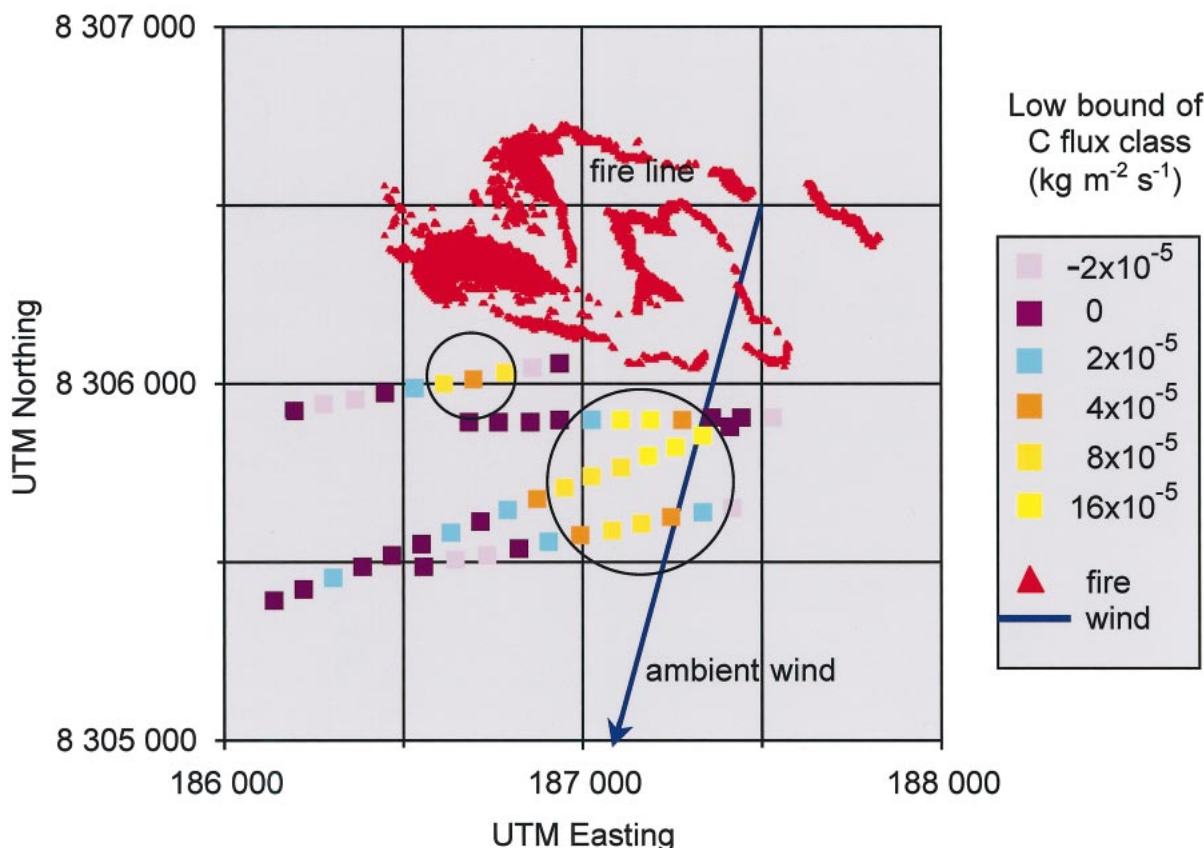


FIG. 10. Map of vertical carbon flux (depicted as in Fig. 7) for the plume of the 1992 Serra do Maranhão fire. The approximate locations of the cores of primary and secondary plumes are indicated by circles. The low bound of carbon flux progresses as follows:  $-2 \times 10^{-5}$ ,  $0$ ,  $2 \times 10^{-5}$ ,  $4 \times 10^{-5}$ ,  $8 \times 10^{-5}$ ,  $16 \times 10^{-5}$   $\text{kg}\cdot\text{m}^{-2}\cdot\text{s}^{-1}$ .

combination of the whole-fire carbon flux and areal spread rates as in Eq. 6 provides a useful estimate of the fuel consumption rate.

## DISCUSSION

Results presented here are based on the first synoptic, quantitative, and high-resolution measurements of the radiances and temperatures associated with wildland fires. Other multispectral remote-sensing systems, including the Landsat thematic mapper, the advanced very-high resolution radiometer (AVHRR), and airborne MODIS and thematic mapper simulators are critically limited in their ability to make calibrated high-temperature measurements and will commonly saturate over high-temperature targets (Brustet et al. 1991; J. A. Brass, *personal communication*; A. Setzer, *personal communication*), which is to say that the instruments become unresponsive to increasing radiance above some threshold value.

Systems including the AVHRR, imagers of the geostationary operational environmental satellites, and the moderate-resolution imaging spectrometer (MODIS)

have poor resolution in comparison with our airborne measurements and are incapable of discriminating any of the detail of fires depicted here. Furthermore, our measurements of fires in the Cerrado show that average whole-fire flame temperatures vary little with time, despite large fluctuations in temperature and radiant flux density spatially across fire lines, from one line to another, and temporally within specific locations. Thus, coarse-resolution sensors are unlikely to provide much useful detail of flame properties based on time trends in estimated whole-fire temperature, especially when derived from a single infrared wavelength. In the latter case, one cannot estimate both the temperature and emissivity-fractional-area parameter, which we observed to be highly variable and to generally attain values much less than one. Blackbody temperatures estimated from radiance at a single wavelength, regardless of spatial resolution, would be quite low in relation to that of the fire, and critical information regarding fire intensity would be lost. Even multispectral data might be inadequate at resolution equivalent to or coarser than 100 m, since fire radiance at shortwave-



FIG. 11. Sampled slash fire plume near Marabá, Pará, as viewed from the northeast (corresponding to a view from the upper right in Fig. 12). Note the primary tropical forest in the left foreground and the pasture, which had been type converted from tropical forest, on the right. The slashed area contained some standing trees, especially palms.

infrared wavelengths is then confounded with a large signal from solar radiation reflected from the nonfire background. There is large inherent uncertainty as to the background composition (whether ash or vegetation) within a coarse-resolution fire pixel, and resulting temperature estimates represent well neither fire nor background (Riggan et al. 2000).

Our high-resolution measurements in Brazil with the extended-dynamic-range imaging spectrometer show that spreading wildland fires can develop complex thermal environments, even in seemingly simple and relatively uniform fuels, such as those of the grassland-dominated Cerrado. The primary fire line of the Tapera fire initially assumed a shape with several lobes, possibly due to differences in terrain, fuel, or fire buildup near the initial line of ignition. These lobes joined to form a continuous line, which was oriented diagonally to the mean wind, yet the line maintained some history from the earlier configuration with sections, running more perpendicular to the wind, that displayed higher line temperatures and energy release rates. The Serra do Maranhão fire, which was first observed well in progress, also formed a complex of fire lines that waxed and waned with changes of an order of magnitude in radiant flux density or intensity. Of note was a region

of high fire intensity that developed where two fire lines burned together at an acute angle (Fig. 9). Neither the Tapera nor Serra do Maranhão fires developed a classical elliptical shape.

The fires described here represented two distinct and common classes of fire in Brazil: open burning in the dry Cerrado, and clearing fires in slashed forest. They were similar in that each exhibited a gradient of radiometric temperatures across active fire lines with the highest temperatures at the leading edge of those lines. In each fire, there were substantial reaches of fire line at temperatures in the range 1400–1600 K. A distinguishing feature among the three fires was in the relative importance of high-temperature flaming combustion to the overall radiant flux density. In the Serra do Maranhão fire, large and persistent areas of residual combustion were predominant, especially at our earliest observation when only one-third of the radiant flux density was associated with temperatures >1100 K; at the Tapera fire three-quarters of the radiant flux density occurred at such temperatures. Residual combustion at the Serra do Maranhão fire appeared to be aligned with more continuous cover of woody Cerrado vegetation or gallery forests and was coincident with emission rates of carbon monoxide, methane, and hy-

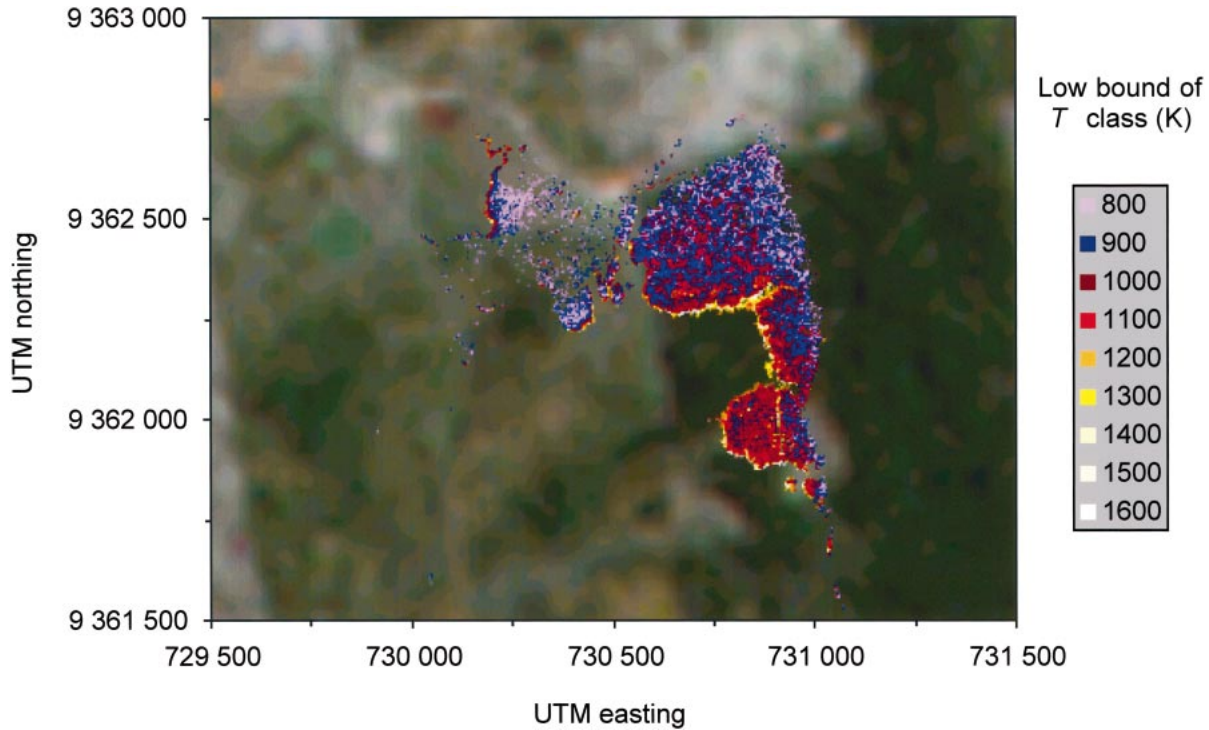


FIG. 12. The radiometric temperatures of the 1992 fire in partially slashed primary tropical forest near Marabá, Pará, at 13:10:27 local time. The background of the graphic is a prefire Landsat Thematic Mapper image with band 7 shown in red, band 5 in green, and band 3 in blue. The slash fire (right of center) is associated with a strong fire front and wide reach of residual combustion. Note the concurrent burning in pasture (left of center) with cooler fire lines and discontinuous residual combustion. The most northerly edge of the fire at the top corresponds to the road visible in Fig. 11.

drocarbons that were large relative to other Cerrado fires we have monitored (Riggan et al., *unpublished manuscript*). The Marabá slash fire generated the greatest combustion-zone depth, ~400 m, with only one-

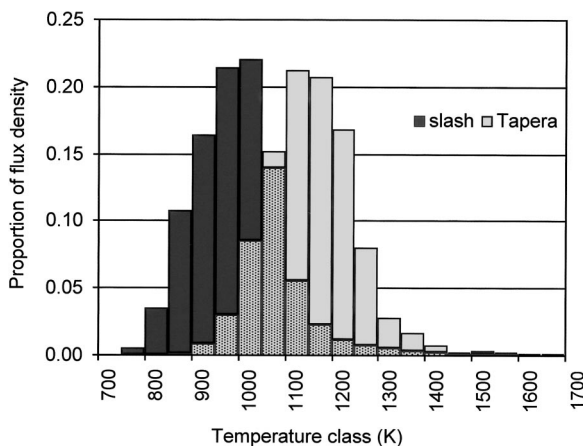


FIG. 13. Comparison of radiant flux density distribution with temperature for the Tapera fire (0:34:19 after first observation) in Cerrado vegetation and the Marabá slash fire (at 13:10:27). Stippling shows the overlap between the two histograms. Energy flux in the Marabá fire is dominated by lower-temperature residual combustion, despite the presence of a highly energetic, high-temperature fire front there.

tenth of its radiant flux density associated with temperatures >1100 K, even though it was partly comprised of a very energetic, high-temperature fire line. There, too, the long fire residence time was associated with high CO emission rates.

The emissivity-fractional-area parameter attained substantially higher values in the Marabá slash fire than observed for the narrow fire lines of the Tapera fire. Although this parameter is expected to be sensitive to the spatial resolution of remote sensing, increasing as sampling scales are reduced in relation to the size and heterogeneity of the flaming front, the large and consistent difference between the fires must have been due to different fire properties, since the Tapera fire, which had the lowest values, was viewed at very high resolution. Ninety-five percent of the radiant flux density from the narrow lines of the Tapera fire was at values of the emissivity-fractional-area parameter <0.26 m<sup>2</sup>/m<sup>2</sup>. In contrast, less than one-third of the radiant flux density from the Marabá slash fire was associated with such values. Indeed, some areas there showed values of the parameter near 1.0, and approximately four percent of the radiance was associated with values >0.8. Such high values are possible only if the associated hot targets have a very high emissivity, as expected for black carbon or soot. Thus, we consider that bulk emissivity is likely very high for the combined system of

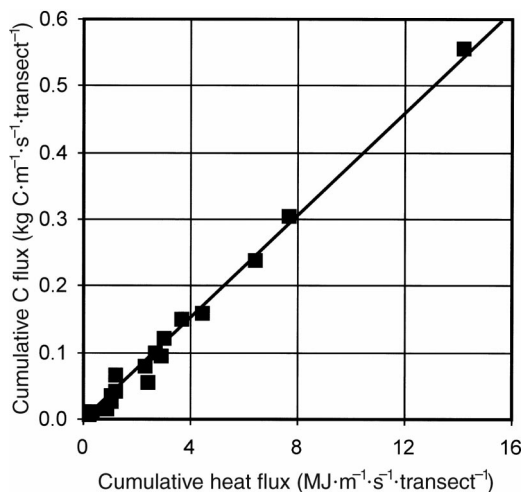


FIG. 14. Relation of carbon flux ( $F_C$ ) to sensible-heat flux ( $Q_s$ ) for a series of aircraft transects through fire plumes in the Brazilian Federal District and State of Pará. Included are observations of the Tapera fire and Marabá slash fire, along with pasture and land-clearing fires observed on 22 September 1992. The regression equation is given by  $F_C = (3.83 \times 10^8)Q_s$ ; confidence limits for the regression coefficient are given by  $\text{Pr}\{3.68 \times 10^8 \leq \beta \leq 3.99 \times 10^8\} \geq 0.95$ ;  $R^2 = 0.99$ .

flames and hot underlying surface, and in regions with low emissivity–fractional-area, such as throughout the Tapera fire, either the instantaneous area of flame within flaming zones is small or the flames have a small optical depth. The result is that, although the wildland fire fronts are of high temperature, they are not especially bright in comparison with a classic blackbody radiator; the Tapera fire, for example, was only one-quarter as bright.

In each of the three fires sampled, plumes extended at least through the depth of the atmospheric boundary layer. Each of the fires was roughly comparable in size, ranging within 43–59 ha at last observation, and our plume sampling was in lower reaches of each plume, at altitudes from approximately one-tenth to one-third of the plume height. Sensible heat and carbon fluxes and the radiant flux density at temperatures  $>1100$  K from the Serra do Maranhão fire were each 1.6 times those from the Tapera fire; fluxes from the Marabá slash fire were seven to eight times those from the Tapera. Thus, as expected, the slash fire consumed fuel at a much greater rate than either of the Cerrado fires. Yet the much greater sensible-heat flux in the Marabá fire generated a peak vertical air velocity of 15.4 m/s in the lower plume, which was comparable to the maximum of 14.7 m/s observed low in the plume of the Tapera fire. However, the high vertical velocities in the Marabá plume were sustained over a much larger area than in the Tapera fire plume, and this allowed heat and carbon fluxes that were several-fold greater.

The results reported here are internally consistent. There was good correspondence between the plume-

based and remote sensing-based estimate of fuel consumption rate for the Tapera fire ( $1.1 \text{ kg/m}^2$ ) and the mean ground-based estimate of biomass loss during burning ( $1.2 \text{ kg/m}^2$ ; Dias 1994). There was also good correspondence between estimated heat and carbon fluxes for the Tapera fire. Specifically, the sum of sensible- and radiant-heat fluxes, as estimated from plume temperature measurements and remote sensing (Table 2), was 90% of that estimated from the carbon flux and an assumed heat of combustion of  $1.55 \times 10^7 \text{ J/kg}$ , as suggested for tropical savanna vegetation by Griffin and Friedel (1984). The maximum near-ground thermocouple temperature recorded was in the lower range of remotely sensed flame temperatures, but a strict comparison was not possible because the thermocouple responds to its own energy balance and this must differ markedly from that of radiating soot particles in flames.

High-temperature regions within observed fire lines often encompassed several contiguous pixels and were at or near the leading edge, but not uniquely located with respect to remote sensing scan lines. Thus, they do not appear to be related to high noise levels or measurement artifacts in the remote-sensing signal. Although we have no concurrent measurements of a fire from two altitudes, there is an indication that sampling altitude did have some effect on estimated fire temperatures. Higher altitudes tended to map smaller regions of high temperature within fire lines, as might be expected if heterogeneous, multiple-temperature regions are included in the resultant, larger pixels.

The remote-sensing methodology described here provides synoptic measures of fuel consumption, energy release, and rates of spread by active wildland fires that could be important in fire modeling and understanding fire behavior. Currently operational fire models including the two-dimensional FARSITE (Finney 1998) are largely based on laboratory-scale experiments (Rothermel 1972) with narrow fuel beds and flame lengths on the order of one meter; their application to fires with high rates of energy release and conditions producing flames many meters in length requires a wide and questionable extrapolation. More complex models have been developed to describe transport of mass, momentum, and energy in a fire environment (Linn 1997). These explicitly describe interactions of fire with the atmosphere, including fire-generated winds, and provide a means to simulate fire behavior in nonhomogeneous fuels and terrain and rapidly changing weather. Application and improvement of both classes of models requires initiation with realistic fuel consumption data and validation with spatially resolved observations of wildfires under realistic settings and scales.

Fire remote sensing provides an efficient and practical means to document actual response of wildfires to applied fuel treatments by contrasting, for example, the rate of spread by a single wildfire and its intensity through different age classes in chaparral or managed

and unmanaged forest fuels. Such information is needed to explain observed fire ecological effects and in strategic planning to define appropriate levels of fuel management to reduce ecological and societal losses from catastrophic fire.

Our methodology can contribute to estimates of fire emissions, which especially in the tropics might be a strong source of greenhouse gases that are important in the global radiation balance (Crutzen and Andreae 1990). At both local and regional scales, emissions can be estimated from the time-integrated product of the areal rate of fire occurrence, the biomass consumption rate per area of land burned, and trace gas or particulate emissions per unit of biomass consumed.

Here, we have shown the efficacy of remote sensing for estimating the second factor in this product: the areal biomass consumption rate. For the disparate classes of fires measured here, remote-sensing estimates of fire geometry, the emissivity–fractional-area parameter, and temperature provided a useful and consistent estimator of sensible-heat flux from flaming combustion. Carbon flux was linearly related to sensible-heat flux, so carbon flux could be similarly estimated by remote sensing. Furthermore, remote sensing can meet an important requirement for large-scale emissions estimates, i.e., an ability to efficiently sample a large number of fires over the extant and complex range of fire conditions, which includes a variety of ecosystem types, fuel loading, and fuel moisture. In tropical ecosystems, this range would necessarily include burning in wetlands, standing tropical forest, pasture, and logging slash. In many of these situations, the fuel consumption rate would be difficult to establish by ground-based methods that estimate mass loss during burning, since fuel loading and consumption can have an inherently large spatial variance, and ground-based sampling is labor-intensive and limited in scope and can ignore potentially important fuels by a priori assumptions about what will be burned under a given set of conditions. Remote sensing of fuel consumption by active fires appears to be the most advantageous means to make the required large-scale estimates.

#### CONCLUSION

We have made synoptic, high-resolution measurements by airborne remote sensing of radiances and intensity of wildland fires in tropical savanna and forest of Brazil and combined these with in situ plume measurements to develop estimators for fire energy and carbon fluxes and fuel consumption. The methodology provides a means to understand the ecological and environmental effects of wildland fires, which can develop complex thermal environments. Even in relatively simple savanna fuels, radiant flux density, which is a measure of intensity, ranged over an order of magnitude. Fire lines showed gradients of temperature with substantial reaches  $>1400$  K. A fire in partially slashed tropical forest developed both a high-intensity fire front

and an extensive reach of residual combustion. The distribution of radiant flux density with temperature provided a whole-fire measure that reflected the relative importance to overall energy flux of high-intensity flaming and residual combustion. Observed fire lines attained high temperatures, but generally low values of a computed emissivity–fractional-area parameter; thus, at short-wave infrared wavelengths, they were not especially bright in comparison with a blackbody model. The methodology is expected to have wide application for understanding and modeling fire behavior, in tactical fire operations (especially by showing the relation of fire fighters to areas of critical fire behavior), in strategic planning to manage fire environmental impacts, and in understanding the potentially global role of fire emissions in climate change.

#### ACKNOWLEDGMENTS

This research has been supported by the Instituto Brasileiro do Meio Ambiente e dos Recursos Naturais Renováveis; the U.S. Forest Service, International Programs and Global Change Research Program; the U.S. Agency for International Development, Global Change Program; the USDA Foreign Agricultural Service, Research and Scientific Exchange Division; the NASA Process Studies Program; the National Center for Atmospheric Research; and the Instituto Brasileiro de Geografia e Estatística. The research was made possible by contributions from James Allen, John Arvesen, Diane Bellis, Edward Hildum, Brad Lobitz, Larry Radke, and Captain José Ramos. For their personal support, we wish to thank especially Enoch Bell, Bráulio F. S. Dias, Iracema Gonzales, Helena Lucarelli, Eduardo Martins, Valdis Mezainis, Whetten Reed, Jeff Sirmon, and Eric Stoner.

Trade names, commercial products, and enterprises are mentioned solely for information. No endorsement by the U.S. Government is implied.

#### LITERATURE CITED

- Brustet, J. M., J. B. Vickos, J. Fontan, A. Podaire, and F. Lavenu. 1991. Characterization of active fires in west African savannas by analysis of satellite data: Landsat Thematic Mapper. Pages 53–60 in J. S. Levine, editor. Proceedings of the Chapman Conference on global biomass burning: atmospheric, climate, and biospheric implications. MIT Press, Cambridge, Massachusetts, USA.
- Crutzen, P. J., and M. O. Andreae. 1990. Biomass burning in the tropics: impact on atmospheric chemistry and biogeochemical cycles. *Science* **250**:1669–1678.
- DeBano, L. F., P. H. Dunn, and C. E. Conrad. 1977. Fire's effect on physical and chemical properties of chaparral soils. Pages 65–74 in H. A. Mooney and C. E. Conrad, editors. Proceedings of the symposium on the environmental consequences of fire and fuel management in Mediterranean ecosystems. U.S. Forest Service (USFS) General Technical Report WO-3. USFS, Washington, D.C., USA.
- Dias, I. F. O. 1994. Efeito da queima no regime térmico do solo e na produção primária de um campo limpo de cerrado. Thesis. Universidade de Brasília, Brasília, Distrito Federal, Brasil.
- Dunn, P. H., and L. F. DeBano. 1977. Fire's effect on biological and chemical properties of chaparral soils. Pages 75–84 in H. A. Mooney and C. E. Conrad, editors. Proceedings of the symposium on the environmental consequences of fire and fuel management in Mediterranean ecosystems. U.S. Forest Service General Technical Report WO-3. USFS Washington, D.C., USA.

- Finney, M. A. 1998. FARSITE: Fire Area Simulator—model development and evaluation. U.S. Forest Service Research Paper RMRS-RP-4. USFS Rocky Mountain Research Station, Fort Collins, Colorado, USA.
- Griffin, G. F., and M. H. Friedel. 1984. Effects of fire in Central Australia rangelands. I. Fire and fuel characteristics and change in herbage and nutrients. *Australian Journal of Ecology* **9**:381–393.
- Lenschow, D. H., and P. Spyers-Duran. 1989. Measurement techniques: air motion sensing. National Center for Atmospheric Research (NCAR) Bulletin 23. NCAR Research Aviation Facility, Boulder, Colorado, USA.
- Linn, R. R. 1997. A transport model for prediction of wildfire behavior. Los Alamos National Laboratory (LANL) Report LA-13334-T. LANL, Los Alamos, New Mexico, USA.
- Liou, K. 1980. An introduction to atmospheric radiation. International Geophysics Series. Volume 26. Academic Press, London, UK.
- Matson, M., and J. Dozier. 1981. Identification of subresolution high temperature sources using a thermal IR sensor. *Photogrammetric Engineering and Remote Sensing* **47**:1311–1318.
- Moreno, J. M., and W. C. Oechel. 1994. Fire intensity as a determinant factor of postfire plant recovery in southern California chaparral. Pages 26–45 in J. M. Moreno and W. C. Oechel, editors. *The role of fire in Mediterranean-type ecosystems*. Springer-Verlag, New York, New York, USA.
- National Center for Atmospheric Research. 1990. *The King Air: overview and summary of capabilities*. National Center for Atmospheric Research Bulletin 2. NCAR, Research Aviation Facility, Boulder, Colorado, USA.
- Ottmar, R. D., R. E. Vihnanek, H. S. Miranda, M. N. Sata, and S. M. Andrade. 2001. Stereo photo series for quantifying Cerrado fuels in central Brazil. Volume 1. U.S. Forest Service, Pacific Northwest Research Station, Portland, Oregon, USA.
- Riggan, P. J., J. A. Brass, and R. N. Lockwood. 1993. Assessing fire emissions from tropical savanna and forests of central Brazil. *Photogrammetric Engineering and Remote Sensing* **59**(6):1009–1015.
- Riggan, P. J., J. W. Hoffman, and J. A. Brass. 2000. Estimating fire properties by remote sensing. Proceedings of the IEEE Aerospace Conference, paper no. 519. IEEE, Aspen, Colorado, USA.
- Riggan, P. J., F. H. Weirich, L. F. DeBano, P. M. Jacks, R. N. Lockwood, C. Colver, and J. A. Brass. 1994. Effects of fire severity on nitrate mobilization in watersheds subject to chronic atmospheric deposition. *Environmental Science and Technology* **28**(3):369–375.
- Rothermel, R. C. 1972. A mathematical model for predicting fire spread in wildland fuels. U.S. Forest Service, Intermountain Forest and Range Experiment Station, Ogden, Utah, USA.
- Stull, R. B. 1988. An introduction to boundary layer meteorology. Kluwer, Dordrecht, The Netherlands.
- Van Wagner, C. E. 1973. Height of crown scorch in forest fires. *Canadian Journal of Forest Research* **3**:373–378.
- Wells, W. G., II. 1981. Some effects of brushfires on erosion processes in coastal southern California. Erosion and sediment transport in Pacific rim steeplands. *International Association of Hydrological Sciences Publication* **132**:305–342.